

Theoretical Study of Zeolite-Catalyzed Dimethoxymethane Carbonylation to Methyl Methoxyacetate

Vladimir Shapovalov and Alexis T. Bell*

Department of Chemical Engineering, University of California, Berkeley, California 94720-1462

Received: June 29, 2010; Revised Manuscript Received: September 3, 2010

The gas-phase carbonylation of dimethoxymethane (DMM) to form methyl methoxyacetate (MMAc) can be catalyzed by acid zeolites. This reaction is a critical step in the synthesis of monoethylene glycol (MEG), a widely used chemical, from synthesis gas. The mechanism of DMM carbonylation occurring on H-MFI and H-FAU zeolites has been investigated using density functional theory. We find that the reaction involves three steps: initiation via reaction of zeolite protons with DMM to form methoxymethoxy species, carbonylation of the resulting species, and subsequent methylation of the resulting acyl species. Both the carbonylation and methylation processes proceed via carbocationic transition states that are stabilized by the framework O atoms of the zeolite. The activation barriers for carbonylation are similar in both zeolites, but the barriers for methylation differ significantly. Energy decomposition analysis indicates that a combination of the pore size and of the flexibility of the reactive species gives rise to the differences in reactivity between the zeolites. The effect of basis set superposition was assessed using a 6-311++G(3df,3pd) basis set. This effect depends strongly on the gas-phase molecules involved but very weakly on the zeolite framework, and its estimate can be transferred from one zeolite to another to reduce the computational expense of such simulations.

1. Introduction

Monoethylene glycol (MEG) is a high-volume commodity chemical widely used as antifreeze and as an intermediate in the manufacturing of synthetic fibers, foams, and plastics. At present MEG is made exclusively by the epoxidation of ethene and the subsequent hydration of the resulting ethylene oxide.¹ Since the demand for ethylene exceeds its supply and its price is rising, there is interest in considering alternative starting materials. A potentially attractive candidate is synthesis gas, a mixture of CO and H₂, which can be obtained by gasification of a variety of carbon sources, such as methane, coal, and biomass. One potential route for the production of MEG from syngas is shown in Figure 1. In the first step, methanol is produced by the hydrogenation of CO, which is then partially oxidized to produce formaldehyde. The latter product can then react with methanol to produce dimethoxymethane (DMM). The carbonylation of DMM produces methyl methoxyacetate (MMAc), which can be readily converted to MEG in two additional steps. The critical step in this scheme is the carbonylation of DMM. In a recent study we have shown that a high selectivity to MMAc can be achieved by carrying out the carbonylation step in the gas phase using H-FAU zeolite as the catalyst.² Other zeolites, such as H-MFI, will also catalyze this reaction but with a lower selectivity and a greater tendency to promote the disproportionation of DMM to form dimethyl ether and methyl formate.³

We have recently proposed a mechanism for MMAc synthesis from CO and DMM based on in situ infrared studies and measurements of reaction kinetics.^{3,4} As seen in Figure 2, the first step in this sequence is the reaction of DMM with a Brønsted acid proton to form methanol and a methoxymethoxy group. The occurrence of this step is supported by in situ IR spectroscopy, which shows the disappearance of the Brønsted acid proton and the concurrent appearance of methoxymethoxy species, and by the transient formation of methanol. The next

step in the process is the carbonylation of the methoxymethoxy species to produce methoxyacetyl species. Evidence for the latter species was also obtained from in situ IR observations. The final step in the sequence is methylation of the methoxyacetyl species to form MMAc and restoration of the methoxymethoxy species. Consistent with this mechanism, the rate of MMAc formation in both FAU and MFI is positive order in CO and nearly zero order in DMM. It was further observed that the rate of MMAc formation is proportional to the concentration of the methoxyacetyl species, as would be expected based on the mechanism presented in Figure 2.

The aim of this study was to understand how zeolite framework structure affects the activation barriers for the two critical steps of the mechanism, the carbonylation of DMM (reaction 2 in Figure 2) and the methylation of the resulting methoxyacetyl intermediate (reaction 3 in Figure 2). These objectives were pursued using a large molecular cluster representation of the active site and the surrounding zeolite framework and were carried out using density functional theory (DFT). The results of this work reveal that the zeolite structure strongly influences the configuration of reaction intermediates and the activation barriers for reactions 2 and 3. Our studies also reveal that the transition states for these two processes are carbocationic in nature and that the oxygen atoms of the zeolite framework play an important role in stabilizing the transition state.

2. Computational Approach

The catalytically active center, a Brønsted acid proton, and a portion of the surrounding zeolite framework were represented by molecular clusters terminated with H atoms. As shown in Figure 3 the cluster used for MFI included 44 T sites (tetrahedral sites) and that for FAU included 36 T sites. The size of each cluster was chosen to represent the confinement effect of the zeolite cages or channels. The location of Al in MFI is not

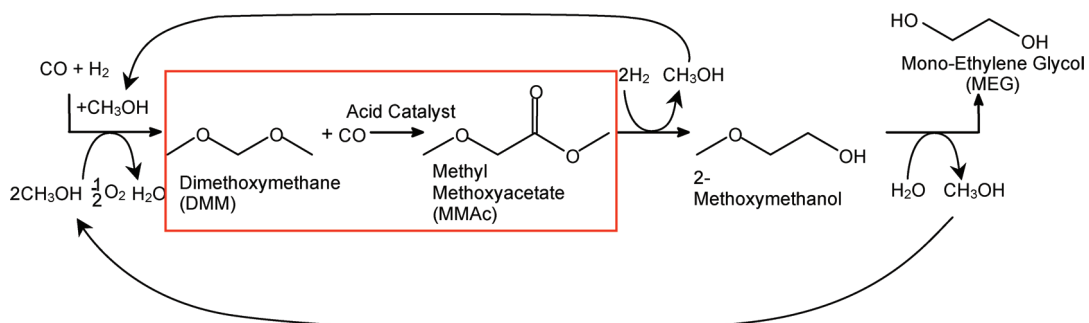


Figure 1. Path to production of MEG from synthesis gas. Outlined in the box is the reaction investigated in this paper.

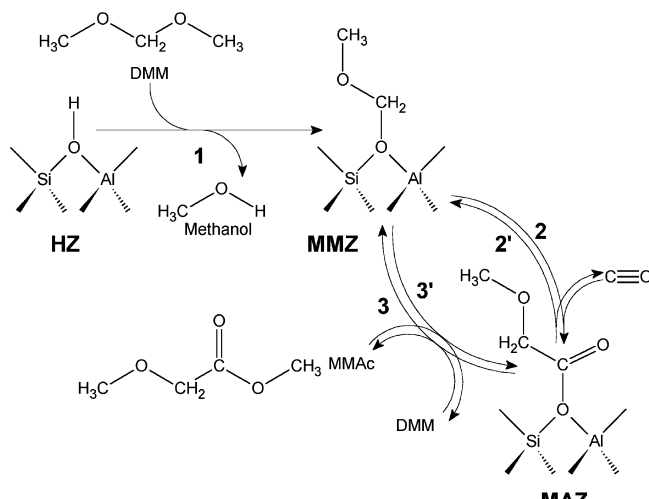


Figure 2. Proposed mechanism of DMM carbonylation catalyzed by acid zeolites.

uniquely defined;^{5,6} nevertheless, there is some evidence that Al siting is not random and that the T12 site is preferred.^{7,8} Based on these findings and other theoretical studies on H-MFI,^{9–11} the T12 position was chosen as a representative T site, and the Brønsted acid proton was placed at O36 so that it faced the channel intersection. In FAU all T sites are equivalent and the only choice is the placement of the proton on one of the four O atoms attached to the Al atom. As seen in Figure 3, the proton was placed so that it faced the supercage. The Si atoms at the edge of both clusters were terminated by H atoms.

The initial positions of the atoms in the zeolite structures were taken from the database included in Materials Studio, version 4.3.¹² To obtain the reactant geometries, the following method was used. For the acid zeolites, the terminating Si atoms were frozen in their crystallographic positions, and the terminating H atoms, the acidic H, the Al, and all O atoms were relaxed.

Following this step, the positions of all atoms in the cluster representing the zeolite were frozen, with the exception of those atoms located within the second coordination shell of the active site and any organic, which were allowed to relax. We found that during chemical transformations the displacement of the atoms in the second coordination shell were small, and therefore, we believe that fixing the positions of the atoms outside the second coordination shell has a minimal effect on the optimized structures and energies. DMM and MMAc molecules have many degrees of freedom. Therefore, a relaxed scan of the potential energy surface was performed, where dihedral angles were scanned in increments of 30°, and all remaining degrees of freedom were optimized to an energy minimum.

All structures and vibrational spectra were computed using density functional theory. For technical reasons calculations were done using both the DMol³ module of the Materials Studio¹³ and Gaussian 03.¹⁴ The most challenging part of the calculations was optimization of the transition states. Utilization of the QST3 method in Gaussian resulted in poor estimates and convergence when started from reactant and product structures. We were able to obtain solutions faster and more reliably using the QSTN method as implemented in DMol³. Unfortunately, DMol³ does not optimize to the true saddle point along the reaction coordinate. Therefore, DMol³ was used to locate approximate transition states using the LST/QST search method and then to confirm that there were no other transition states, using the built-in variant of the Nudged Elastic Band method. The structures obtained with DMol³ were used as starting points for relaxation in Gaussian 03. Transition states were refined in Gaussian 03 using the Berny optimization option and then confirmed by computing the Hessian numerically using displacements of only the atoms belonging to the active sites, which are comprised of the Al atom and its first two coordination shells, and all organic moieties. Multiple Hessian evaluations were required to achieve the optimal geometry with only one imaginary vibrational frequency. For this reason up to two months of wall time were

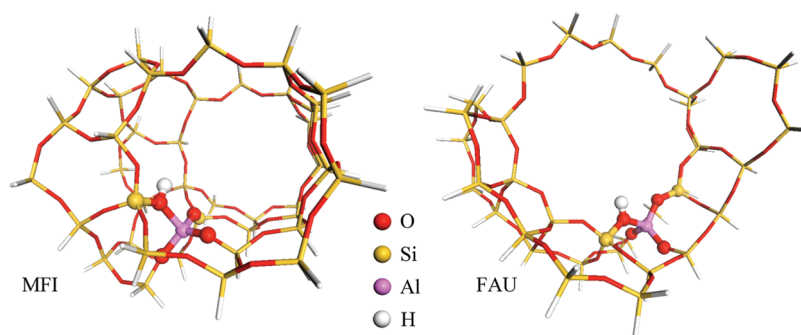


Figure 3. Models for MFI and FAU zeolites. Spheres show zeolite atoms that are allowed to relax during optimizations. The acid site is shown by adsorbed hydrogen atom.

TABLE 1: Stability of Conformers of Adsorbed Methoxymethoxy As the Energy Change during the Initiation Step and of Conformers of Adsorbed Methoxyacetyl As the Energy Change during the Carbonylation Step^a

conformers	MFI sinusoidal channel	MFI straight channel	FAU
Methoxymethoxy			
conformer 1	-3	5	23
conformer 2	8	12	28
conformer 3	N/A	23	38
Methoxyacetyl			
conformer 1	-52	-67	-40
conformer 2	-30	-62	-31
conformer 3	N/A	50	N/A

^a The conformer structures are given in the Supporting Information. N/A (not applicable): a stable conformer was not found. Values are in kJ/mol, computed at the B3LYP/6-31G* level.

necessary in order to obtain a transition state using eight CPUs on an SGI Altix 370 computer.

For DMol³ calculations, we used the PBE functional and the built-in numerical double ζ basis set with the effective core potentials and polarization functions (DNP), with custom cutoff radius of 5.0 Å. Gaussian 03 was used to relax geometric structures obtained in DMol³ calculations, to verify the Hessian structure of the optimized transition states, and to compute the vibrational spectra. These calculations were done using the B3LYP functional with a 6-31G* basis set and ultrafine integration grid. All energies were zero-point corrected. Because this basis set is rather modest by modern standards, the effect of a larger basis set was investigated by performing single-point calculations with the 6-311++G(3df,3pd) basis set on all atoms, except the terminating H, for which the 6-31G set was retained. Basis set superposition error (BSSE) was not estimated explicitly. BSSE in general diminishes with larger basis sets. BSSE was found to be below 1 kJ/mol in a calculation of an ionic liquid ion pair at the B3LYP/6-311++G(d,p) level performed by P. Hunt and I. R. Gould,¹⁵ where it was explicitly evaluated

using the counterpoise method. Therefore, we expect the BSSE to be below the accuracy of the computational method for the 6-311++G(3df,3pd) basis set.

Calculations were performed on an SGI Altix 3700 cluster at the University of Illinois at Urbana–Champaign, which is a part of the Teragrid system, and on a Beowulf type cluster at the College of Chemistry at the University of California, Berkeley.

3. Results and Discussion

As noted in the Introduction (see Figure 2), the carbonylation of DMM is initiated by the reaction of DMM with the Brønsted acid center in the zeolite to produce methanol and an adsorbed methoxymethoxy group. The computed change in the electronic energy for this step is reported in Table 1 at the B3LYP/6-31G* level of theory.

In the case of MFI, two conformers of the methoxymethoxy group were identified in the sinusoidal channel and three in the straight channel. Formation of conformer 1 in the sinusoidal channel is slightly exothermic, whereas formation of conformer 2 in this channel is endothermic. As seen from Table 1, in the straight channel the energies of formation of all three conformers are endothermic. The structures of the lowest energy conformers in the sinusoidal and straight channels are shown in Figure 4a, b, and structures for the remaining conformers are given in the Supporting Information. By contrast, in FAU the formation of all three methoxymethoxy conformers are endothermic. Figure 4c illustrates the structure of the lowest energy conformer in FAU, and the structures of the other two conformers are given in the Supporting Information.

It is important to note that the endothermicity of forming methoxymethoxy species, which can be as high as 37 kJ/mol, does not preclude the formation of these species. During the initial exposure of the acid form of the zeolite, methanol formed as the byproduct of the reaction is swept out of the reactor and hence is not available to back-react with newly formed methoxymethoxy species. Since methanol is not produced as a

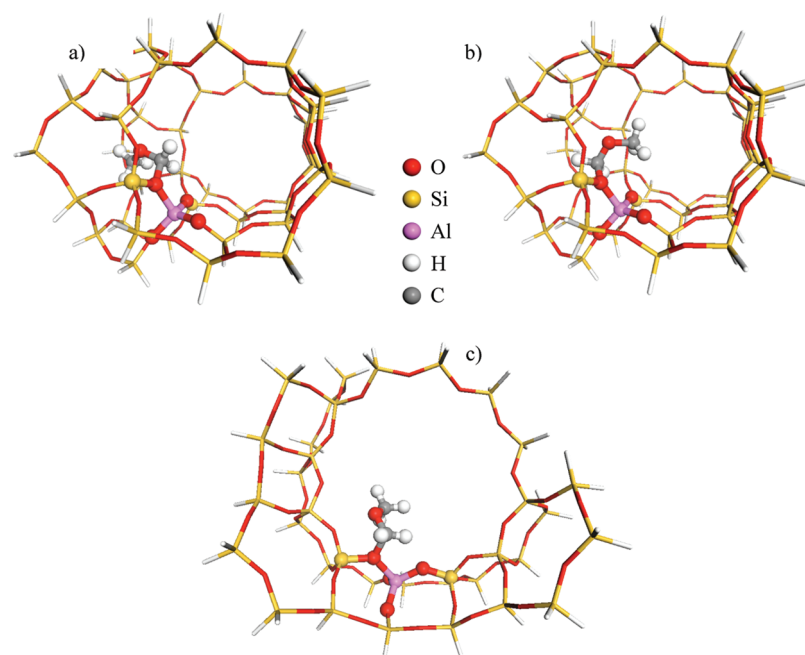


Figure 4. Lowest energy isomers for methoxymethoxy species adsorbed on acid MFI with orientation toward the sinusoidal (a) and straight (b) channel and also adsorbed on FAU (c).

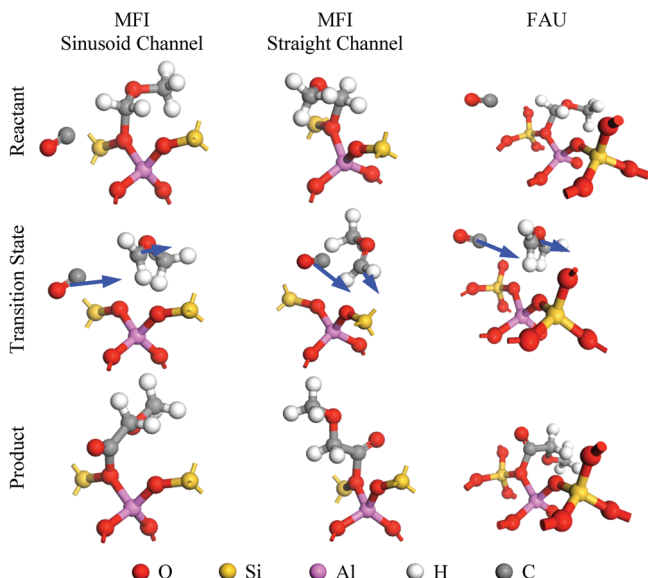


Figure 5. Reactants, transition states, and products of the carbonylation step in the MFI sinusoidal (left column) and straight (middle column) channels and in FAU (right column). In the transition state panels, the arrows roughly indicate the atomic displacements corresponding to the imaginary frequencies.

TABLE 2: Energies (in kJ/mol) of the Intermediates and Transition States for DMM Carbonylation^a

composition	MFI sinusoidal channel	MFI straight channel	FAU
DMM, CO, $\text{C}_2\text{H}_5\text{O}-\text{Z}$	0	0	0
DMM, $[\text{CO}-\text{C}_2\text{H}_5\text{O}-\text{Z}]^\ddagger$	55	64	68
DMM, $\text{C}_2\text{H}_5\text{OCO}-\text{Z}$	-28	-21	-33
$[\text{DMM}-\text{C}_2\text{H}_5\text{OCO}-\text{Z}]^\ddagger$	21	47	-17
MMAC, $\text{C}_2\text{H}_5\text{O}-\text{Z}$	-73	-89	-80

^a Zero-point energies are included. DMM and MMAC energies correspond to free molecules in vacuum. "Z" designates the zeolite cluster. Energy is the sum for all species listed in the composition column. Energies were computed at the B3LYP/6-31G* level.

byproduct of DMM carbonylation, the methoxymethoxy group is stable to back-reaction, i.e., the reverse of reaction 2.

The formation of MMAC begins with the carbonylation of the methoxymethoxy group (see Figure 2). Figure 5 illustrates the structures of the reactant, transition, and product states for this process occurring in MFI and FAU. In the case of MFI, two carbonylation scenarios are shown, one occurring in the sinusoidal channel and the second occurring in the straight channel. As discussed below, and seen in the video clip presented in the Supporting Information, the methoxymethoxy group moves between being positioned in the sinusoidal channel and in the straight channel during the formation of each molecule of MMAC. The video is an interpolation between the stationary points on the potential energy surface, as the intrinsic reaction coordinate path could not be computed with a partly frozen cluster. Two turns around the catalytic cycle (i.e., formation of two molecules of MMAC) are required to restore the position of the methoxymethoxy species to its original orientation.

Table 2 lists energies for the transition and product states computed at B3LYP/6-31G* level, assuming that carbonylation proceeds from the lowest energy conformer of the methoxymethoxy group in each zeolite. It is evident that for both zeolites carbonylation is exothermic, with the exothermicity decreasing in the order MFI(straight) > MFI(sinusoidal) > FAU. The activation energy for carbonylation is 55 kJ/mol for a

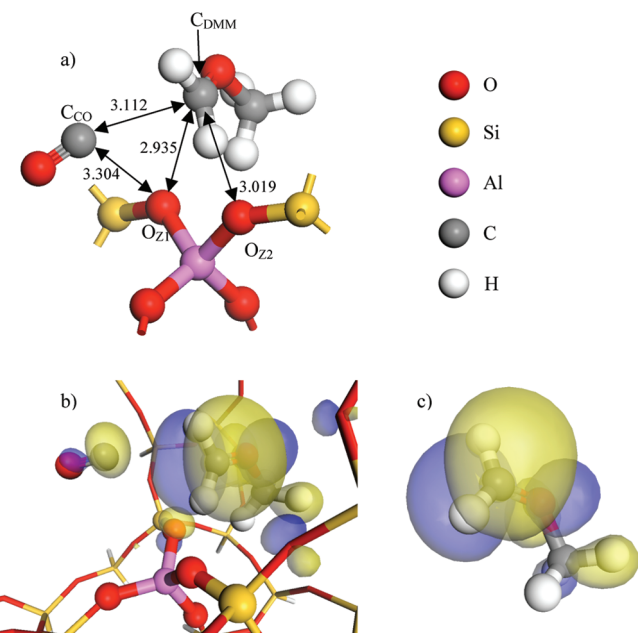


Figure 6. (a) Interatomic distances in the transition state for carbonylation of methoxymethoxy species in the sinusoidal channel of MFI. O_{Z1} and O_{Z2} are the closest oxygen atoms of the zeolite. (b) Lowest unoccupied orbital of the transition state structure for the carbonylation step in MFI, sinusoidal channel. (c) Lowest unoccupied orbital of a free methoxymethyl cation.

methoxymethoxy group located in the sinusoidal channel of MFI, 64 kJ/mol for a methoxymethoxy group located in the straight channel of MFI, and 68 kJ/mol for a methoxymethoxy group located in FAU.

There are examples of reactions where the intermediate adsorbs on the zeolite prior to forming a transition state, such as dehydrogenation of methanol in alkali cation exchanged zeolites.¹⁶ We have made attempts to determine whether CO first adsorbs at or near the adsorbed methoxymethoxy group prior to its insertion in the O–C bond of that species. These calculations failed to reveal a bound CO state for any starting configuration, suggesting that the carbonylation of the methoxymethoxy group is best described as a Rideal–Eley process involving bound and unbound reactants. The NEB calculations carried out with DMol³ show that the methoxymethoxy group first dissociates from the oxygen atom of the zeolite and then reacts with a free CO molecule located in the vicinity of the methoxymethoxy group. Thus, the presence of CO does not induce the dissociation of the methoxymethoxy group from the zeolite.

The transition state for the carbonylation step is best described as an association of CO with the methoxymethyl carbocation formed by the dissociation of the methoxymethoxy group from the zeolite. The vibrational mode corresponding to the imaginary frequency is illustrated by arrows in Figure 5. The methoxymethyl cation rocks from side to side between the two zeolite oxygen atoms connected to the Al (O_{Z1} and O_{Z2}), and the CO molecule center of mass moves toward the carbon of the CH₂ group in the methoxymethyl cation. The cationic nature of methoxymethyl species is confirmed by the planar trigonal structure of the carbon atom and comparison of the molecular orbitals of this structure with those of the corresponding carbocation in vacuum. The orbital plot presented in Figure 6 shows that the carbocation is stabilized in three ways: by the oxygen atom of the methoxy group, by the methyl group, and by the oxygen atoms of the zeolite framework. These findings

TABLE 3: Properties of the Carbonylation and Methoxylation Transition States, in Å^a

atomic pair	MFI sinusoidal channel	MFI straight channel	FAU
Carbonylation ^b			
imaginary frequency, cm ⁻¹	50.14	84.65	12.44
C _{DMM} —C _{CO}	3.112	2.476	2.862
C _{DMM} —O _{Z1}	2.935	2.846	2.983
C _{DMM} —O _{Z2}	3.019	3.106	3.170
C _{CO} —O _{Z1}	3.304	2.924	3.439
C _{CO} —O _{Z2}	4.028	3.390	4.557
Methoxylation ^c			
imaginary frequency, cm ⁻¹	21.29	N/A ^d	24.25
O _{Methox} —C _{DMM}	1.743	1.604	1.828
O _{Methox} —C _{Mac}	1.522	1.603	1.392
C _{Mac} —O _{Z1}	3.902	3.503	4.958
C _{DMM} —O _{Z1}	5.078	3.600	2.713

^a O_{Z1} and O_{Z2} refer to the oxygen atoms bound to the Al atom of the zeolite, O_{Z1} being the atom on which methoxymethoxy is adsorbed. Structures were optimized at the B3LYP/6-31G* level.

^b Refer to Figure 6 for an explanation of these atom pairs. ^c Refer to Figure 8 for an explanation of these atom pairs. ^d Optimization was stopped due to the energy changes less than 10⁻⁷ hartree between optimization steps.

are consistent with those of Boronat et al.,¹⁷ who carried out a theoretical study of the carbonylation of dimethyl ether (DME) catalyzed by MOR. These authors demonstrated that the carbonylation proceeds via a transition state structure that involves the association of uncoordinated CO with a carbocation formed by the dissociation of a methoxy group present on MOR. The activation energy for this process was calculated to be 80 kJ/mol. The higher value of the activation energy for carbonylation of a methoxy versus a methoxymethoxy group (55 and 64 kJ/mol) reflects the more favorable stabilization of the methoxymethyl carbocation formed in the latter case.

The structure of the transition state formed in MFI (see Figure 6a) displays large distances ($\sim 3 \text{ \AA}$) between the atoms forming and breaking the bonds (e.g., C_{CO}—O_{Z1}, C_{CO}—C_{DMM}, C_{DMM}—O_{Z1}, and C_{DMM}—O_{Z2}). The specific values of these bonds are listed in Table 3. Subtle differences are seen between the geometries of the transition states formed in the straight versus the sinusoid channel. In the former case the oxygen of the zeolite, the carbon of the CH₃OCH₂⁺ cation, and the carbon of the CO form a triangle with sides close to 3 Å each. In the latter case the methyl carbon is found at approximately equal distances from two oxygen atoms connected to the Al atom in the zeolite. This creates a structure that is better described as an irregular trigonal pyramid, or a distorted tetrahedron. The length of the sides of this pyramid is also close to 3 Å (see Figure 6a).

The calculated energies for the carbonylation of methoxymethoxy groups in FAU are listed in Table 2, and critical bond distances associated with the transition state for this process are listed in Table 3. These results indicate that both the energetics of methoxymethoxy carbonylation occurring in FAU and the geometry of the transition state are very similar to those for MFI.

The structures of the species involved in methoxylation of the methoxycetyl species formed upon carbonylation of methoxymethoxy species in MFI and FAU are shown in Figure 7. The initial state for this step involves an adsorbed methoxycetyl group and a free DMM molecule inside the zeolite pore. The reaction starts with methoxycetyl dissociating from the zeolite to form an acyl cation. This cation attracts the lone electron

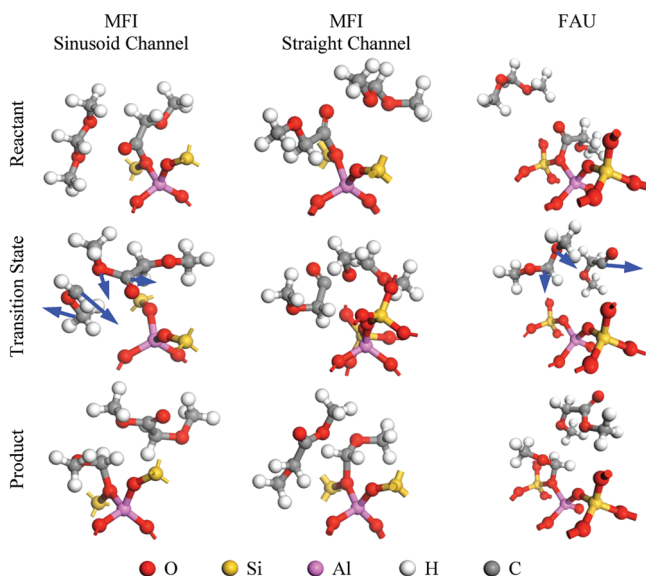


Figure 7. Reactants, transition states, and products of the CH₃O[−] step in the MFI sinusoid (left column) and straight (middle column) channels and in FAU (right column). In the transition state panels the arrows roughly indicate the atomic displacements corresponding to the imaginary frequencies. The transition state in the sinusoidal channel of MFI does not have arrows as the optimization was stopped due to negligible energy changes between optimization steps.

pairs of the oxygen atoms of DMM. One of the two methoxy groups of DMM breaks the bond with DMM and attaches itself to the acyl cation. This produces a MMAc molecule and a methoxymethyl cation. This cation then associates with the zeolite active site. The energies of the products of methoxylation of methoxycetyl species are listed in Table 2. The panels in Figure 7 that show the transition states have arrows indicating the atomic displacement in the vibrational mode corresponding to the imaginary frequency. The atomic displacements in the sinusoidal channel of MFI are such that the methoxymethyl cation rocks in the plane of the flat CH₂ group around the axis roughly passing through the O atom. This motion brings the CH₂ group closer to the oxygen of the MFI framework. The methoxy group shifts toward the methoxycetyl, and both of these groups together rock in and out of the sinusoidal channel. The transition state in the straight channel of MFI never converged to a single imaginary Hessian eigenvalue; however, the energy changes during optimization fell below the prescribed convergence limit, and, consequently, the reaction coordinate could not be identified definitively. In the transition state for methoxylation occurring in FAU, the migrating methoxy group is closer to the gas-phase DMM, but moving away from it. The methoxycetyl fragment moves up and away from the zeolite framework. In all cases the atoms of the zeolite framework gave negligibly small displacements, indicating that the barrier crossing involves a species dissociated from the zeolite. Figure 8 shows a more detailed view of the transition state formed in the sinusoidal channel. It is seen that, similar to carbonylation, the transition state for methoxylation is characterized by large interatomic distances between atoms in the transition state and those in the zeolite. Table 3 lists the principal distances for each of the three transition states shown in Figure 7.

The calculated activation energy for methoxylation of a methoxycetyl group in the sinusoidal channel of MFI is 49 kJ/mol, whereas that for the methoxylation of a methoxycetyl group in the straight channel is 68 kJ/mol. These values are very similar to those determined for carbonylation of methoxymethoxy groups in the same channels, indicating that the

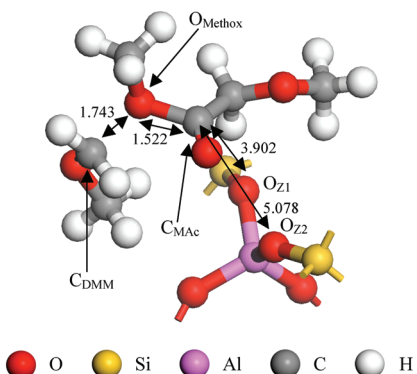


Figure 8. Typical distances in a transition state for methoxylation of methoxyacetyl species in the sinusoidal channel of MFI. O_{Z1} and O_{Z2} are the closest oxygen atoms of the zeolite.

activation energy associated with the formation of a carbocation for both reactions is very similar. In the case of FAU the activation energy for methoxylation of methoxyacetyl groups is 16 kJ/mol, which is significantly lower than that for MFI.

The changes in the enthalpy leading to the formation of MMAc are shown in Figure 9a and 9b for reactions occurring in the sinusoidal channel of MFI and in the supercage of FAU. Both quantities were determined for 373 K, a temperature characteristic of that used in the experimental studies.³ The zero in enthalpy is taken as an adsorbed methoxymethoxy group and one free DMM molecule. Plots of the changes in the enthalpy for the straight channel in MFI are similar to those for the sinusoid channel and are not shown. It is evident from Figure 9 that both the activation barrier for carbonylation of methoxymethoxy and the energy of the resulting acyl species are nearly the same for MFI and FAU. The main difference between

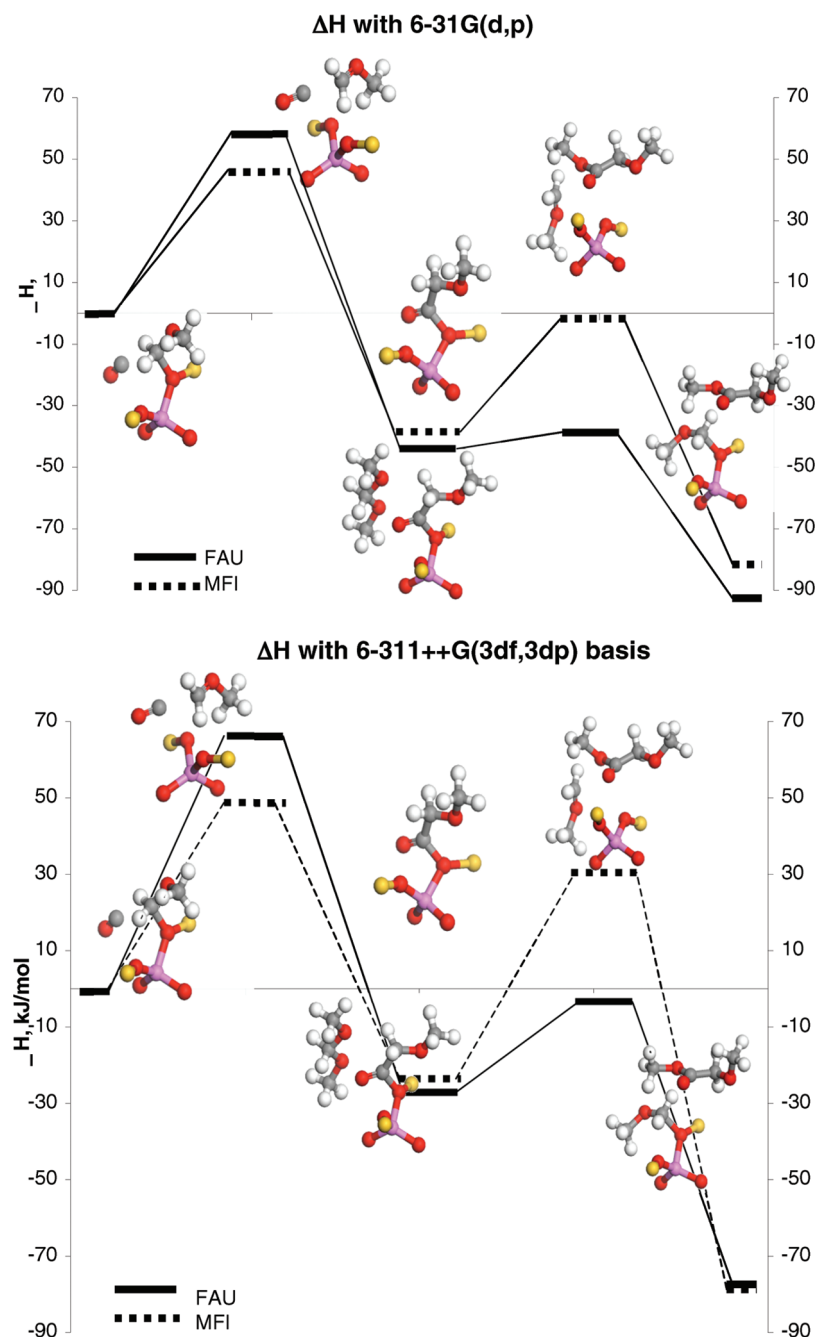


Figure 9. Reaction path for carbonylation of DMM to MMAc. The energy of the product differs between MFI and FAU because only the path for the straight channel of MFI is shown. Top, data computed at the B3LYP/6-31G(d,p) level; bottom, data corrected at the B3LYP/6-311++G(3df,3pd) level.

TABLE 4: Energy Balance for Fitting a Free Methoxy Exchange Transition State Structure into a Zeolite Framework^a

zeolite	conformation strain ΔE_{Conf}	stabilization by framework, ΔE_{Stabl}	sum
Carbonylation			
MFI	19	-418	-399
FAU	10	-395	-384
FAU-MFI	-8	24	15
Methoxylation			
MFI	24	-318	-294
FAU	110	-447	-336
FAU-MFI	86	-129	-42

^a Values are in kJ/mol, computed at the B3LYP/6-31G* level.

the two zeolites is in the activation energy of the methoxylation of the acyl species, with the activation barrier being significantly smaller in FAU than MFI.

Since the activation barrier for methoxylation of the acyl species is significantly lower for FAU than MFI, it is expected that the surface concentration of the acyl species should be higher on MFI than FAU due to the slower rate of removal of these species on MFI. This prediction is completely consistent with *in situ* IR observation, which shows a 10-fold higher concentration of adsorbed acyl species on MFI.³

To understand the observed differences in the activation barrier for the two steps involved in the formation of MMAc, an energy decomposition analysis was performed on the two transition states shown in Figure 9. This was done by first determining the structure for the fully relaxed carbocation transition state in vacuum without the influence of the confinement and stabilization provided by the zeolite. The structure of the transition state was then altered to conform to that found in either MFI or FAU. The computed energy change for this step is designated as ΔE_{conf} . The reformed structure is then placed inside the zeolite framework. This results in stabilization due to the interaction of the carbocationic transition state with the negatively charged cation-exchange site delocalization of the positive charge of the carbocation over the framework oxygen atoms. The difference between the energy of the transition state structure stabilized inside the zeolite and the energies of the separated carbocation and the zeolite framework is designated as ΔE_{Stabl} .

Table 4 shows the conformational strain computed at the B3LYP/6-31G* level. For the carbonylation transition, it is endothermic for both MFI and FAU but is 8 kJ/mol higher for MFI than for the more open structure of FAU. By contrast, the stabilization energy is highly exothermic for both zeolites, and 24 kJ/mol larger for MFI. The sum of ΔE_{conf} and ΔE_{Stabl} is again exothermic, and again stabilization of the transition state for carbonylation of methoxymethoxy species is 15 kJ/mol greater for MFI than FAU.

Energy decomposition analysis give a different picture, however, for the transition state associated with methoxylation of the acyl species. Table 4 shows that, in this case, the strain energy associated with the change in conformation of the transition state is 86 kJ/mol higher for FAU than MFI, but the stabilization energy is 129 kJ/mol higher for FAU than MFI, leading to a net stabilization energy that is 42 kJ/mol greater for FAU relative to MFI.

Thus, energy decomposition analysis demonstrates that the proximity of the carbocationic species to the walls of the zeolite pore has a strong stabilizing effect on these species if they have the freedom to conform to the zeolite structure. It is also seen

TABLE 5: Influence of the Basis Set on the Energies of the Intermediates and Transition States, kJ/mol^a

composition	E(B3LYP/ 6-31G*)	E(B3LYP/ 6-311++G(3df,3dp))	ΔE
	MFI	Sinusoidal	Channel
DMM, CO, C ₂ H ₅ O-Z	0	0	0
DMM, [CO-C ₂ H ₅ O-Z] [‡]	61	64	3
DMM, C ₂ H ₅ OCO-Z	-35	-22	13
[DMM-C ₂ H ₅ OCO-Z] [‡]	13	40	27
MMAc, C ₂ H ₅ O-Z	-61	-57	4
FAU			
DMM, CO, C ₂ H ₅ O-Z	0	0	0
DMM, [CO-C ₂ H ₅ O-Z] [‡]	73	80	7
DMM, C ₂ H ₅ OCO-Z	-41	-26	15
[DMM-C ₂ H ₅ OCO-Z] [‡]	-26	4	30
MMAc, C ₂ H ₅ O-Z	-68	-57	11

^a ZPE not included. DMM and MMAc energies correspond to free molecules in vacuum. "Z" designates the zeolite cluster. Energy is the sum for all species listed in the composition column.

that such stabilization is largest in the case of the transition state for methoxylation occurring in FAU. In fact, favorable electronic interactions between the zeolite framework and the carbocation are sufficiently strong to accommodate its change in conformation relative to that in the vacuum. The electronic stabilization energy is smallest for methoxylation of acyl species occurring in MFI, where the large transition state is modestly strained compared to the structure in vacuum, but the confined space does not allow the transition state to adapt to the pore shape to take the full advantage of the electronic stabilization. In the intermediate case of the carbonylation step, the transition state structure is small, which diminishes the differences imposed by the pore sizes, and has a smaller number of degrees of freedom.

Given the importance of carbocationic transition state stabilization by the oxygen atoms of the zeolite framework on the one hand, and the susceptibility of the small basis sets to the basis set superposition error on the other hand, it was of interest to determine the effects of using a more flexible set with functions of higher angular momentum. The total energy for each stage in MFI and FAU, not including the zero-point energy, is presented in Table 5 for two levels of calculation: B3LYP/6-31G* and B3LYP/6-311++G(3df,3pd). The energy of each stage of the reaction is increased by the larger basis set. This reflects the basis set superposition phenomenon. The initial state corresponds to the most dissociated species. Therefore, the energy of the initial state is lowered more than the energy of any other state, resulting in positive differences for all stages.

We can make two comparisons related to the basis set influence. First, we observe that the increase of the activation energy is larger for methoxylation than for carbonylation. This is due to the energy of the gas-phase DMM being lowered more than the energy of gas-phase CO. Therefore, when CO is absorbed into the transition state the basis set superposition does not have as much of an effect as when DMM forms the methoxylation transition state.

Second, we can compare the influence of the basis set on MFI and FAU models. Table 5 shows that the energy change due to the basis set is similar for both zeolites for the corresponding reaction steps. Therefore, we can conclude that the lowering of the energy of the gas-phase species is responsible for the major part of the effect that the basis set has on the reaction energies. We suggest that in the future studies a significant computational effort can be saved by computing the

energy correction for only one zeolite and applying it to any other zeolite under study.

4. Conclusions

DFT calculations have been performed for DMM carbonylation catalyzed by H-MFI and H-FAU in gas phase. Reaction is initiated by the reaction of Brønsted acid protons with DMM to form methoxymethoxy species. While this process is endothermic, it is promoted by the continual removal of the methanol formed into the gas phase in a flow system. The carbonylation of methoxymethoxy species is reversible and proceeds via a partial dissociation of this species to form a carbocation. Carbonylation of the carbocation by CO does not require preadsorption of CO. The activation energy for carbonylation of methoxymethoxy species is slightly higher for FAU than MFI. MMAc is formed by methylation of the acetyl species formed by carbonylation of methoxymethoxy species. The activation energy for this process is higher for MFI than FAU. The relative coverages by acetyl species and the relative rates of MMAc formation on FAU versus MFI are also described correctly by the analysis presented in this study.

The choice of the zeolite catalyst has the largest effect on the methylation step, with the larger pore size resulting in lower activation energy. The effect is due to a more significant electronic stabilization, providing the transition state has sufficient freedom to conform to the pore shape.

The basis set superposition error depends largely on the gas-phase molecules involved in the reaction. It changes little between MFI and FAU. Therefore, in the future studies of reactivity in zeolites it would be prudent to check whether this correction can be transferred between different zeolites for the purpose of computational savings.

Acknowledgment. This work was supported by the Methane Conversion Cooperative funded by BP. Partial support was also provided by the National Center for Supercomputing Applications under project number CHE090041 and utilized the NCSA

system Cobalt, and by the Molecular Graphics and Computation Facility at the College of Chemistry, University of California Berkeley, under the grant CHE-0233882 from the National Science Foundation.

Supporting Information Available: Zero-point energies of the intermediates and transition states; Cartesian coordinates of the optimized conformers of methoxymethoxy adsorbed on MFI and FAU; animation of the reaction path for carbonylation and methylation steps in MFI. This material is available free of charge via the Internet at <http://pubs.acs.org>.

References and Notes

- (1) *Applied Industrial Catalysis*; Leach, B. E., Ed.; Academic Press: New York, 1983; Vol. 1.
- (2) Celik, F. E.; Kim, T.; Bell, A. T. *Angew. Chem., Int. Ed.* **2009**, *48*, 4813–4815, S4813/1–S4813/2.
- (3) Celik, F. E.; Kim, T.; Bell, A. T. *J. Catal.* **2010**, *270*, 185–195.
- (4) Celik, F. E.; Kim, T.; Mlinar, A.; Bell, A. T. *J. Catal.* **2010**, in press.
- (5) Sarv, P.; Fernandez, C.; Amoureaux, J.; Keskinen, K. *J. Phys. Chem.* **1996**, *100*, 19223–19226.
- (6) Sklenak, S.; Dedecek, J.; Li, C.; Wichterlová, B.; Gábová, V.; Sierka, M.; Sauer, J. *Angew. Chem.* **2007**, *119*, 7424–7427.
- (7) Olson, D. H.; Khosrovani, N.; Peters, A. W.; Toby, B. H. *J. Phys. Chem. B* **2000**, *104*, 4844–4848.
- (8) Barone, G.; Casella, G.; Giuffrida, S.; Duca, D. *J. Phys. Chem. C* **2007**, *111*, 13033–13043.
- (9) Mentzen, B.; Sacerdote-Peronnet, M. *Mater. Res. Bull.* **1994**, *29*, 1341–1348.
- (10) Brändle, M.; Sauer, J. *J. Am. Chem. Soc.* **1998**, *120*, 1556–1570.
- (11) Zygmunt, S. A.; Curtiss, L. A.; Zapol, P.; Iton, L. E. *J. Phys. Chem. B* **2000**, *104*, 1944–1949.
- (12) Materials Studio, version 4.3, Accelrys Software Inc., San Diego, CA.
- (13) Delley, B. *J. Chem. Phys.* **2000**, *113*, 7756.
- (14) Frisch, M. J.; et al. *Gaussian 03*, revision D.01; Gaussian, Inc.: Wallingford, CT, 2004.
- (15) Hunt, P. A.; Gould, I. R. *J. Phys. Chem. A* **2006**, *110*, 2269–2282.
- (16) Kang, L.; Han, K. *Microporous Mesoporous Mater.* **2010**, *127*, 90–95.
- (17) Boronat, M.; Martinez-Sanchez, C.; Law, D.; Corma, A. *J. Am. Chem. Soc.* **2008**, *130*, 16316–16323.

JP106011A